Type of the Paper (Research Article)

Assessment of Hepatotoxicity Induced by Silver Nanoparticles and Possible Therapeutic Effect of Silymarin and Vitamin E in Adult Male Albino Rat: Histological, immunohistochemical and Biochemical study.

Asmaa W.T. Tawfik[1*], Maha K.A. Hussin[1], Abdullah M.S. Abdel Kader[1], Shimaa A.R. Mostafa[1]

[1]Department of Anatomy and Embryology, Faculty of Medicine, Fayoum University, Fayoum, 63514, Egypt.

*Correspondence: Asmaa W.T. Tawfik, AWT00@fayoum.edu.eg, Tel: (002) 01001887347

Received: 17 August, 2024 Reviewed: 1 December, 2024

Accepted: 25 January, 2025 Published online: 6 November, 2025

Abstract:

Introduction: Silver Nanoparticles (AgNPs) have hepatotoxic effects which may be secondary to oxidative stress enhancement. The antioxidants Silymarin and Vitamin E can counteract such effects.

Aim of the study: to clarify the histopathological, immunological and bio-chemical changes that occur in liver following AgNPs administration and the possible therapeutic role of Silymarin and Vitamin E supplementation.

Subjects and Methods: Sixty adult male albino rats were equally divided into: **GI**(normal control) received nothing; **GII**(Sham control): subdivided into subgroup II-A: received normal saline orally for 30 days and subgroup II-B: received 4ml/kg/day of olive oil orally for 30 days; **GIII**(AgNPs treated): received 0.5mg/kg/day of AgNPs I.P. for 30 days; **GIV**(Silymarin treated): injected the calculated dose of AgNPs for 30 days, then starting from the 31st day, was given 100 mg/kg/day of Silymarin orally for 30 days; **GV**(Vitamin E treated): injected the calculated dose of AgNPs for 30 days, then, starting from the 31st day, 400mg/kg/day of vitamin E was given orally for 30 days; **GVI** (Silymarin and Vitamin E treated): injected by the calculated dose of AgNPs for 30 days, then, starting from the 31st day, the calculated doses of silymarin and vitamin E was giving orally concomitantly for 30 days. All specimens were prepared for histological, immunohistochemical and biochemical examinations.

Results: GIII showed variable pathological changes as congestion and dilatation of portal, central veins and sinusoids, mononuclear infiltration, hemorrhage and hepatocyte degenerative changes. Silymarin and vitamin E treated groups displayed relieve of the pathological changes, which were most evident with combined therapy in GVI.

Conclusions: Co-antioxidant therapy exerted the most efficient protective effects against AgNPs induced hepatotoxicity.

Keywords: Liver; Silver Nanoparticles; Silymarin; Vitamin E; BCL-2.

1. Introduction

Current advances in nanotechnology altered how we diagnose, treat and protect against various diseases. Among metallic nano-particles, silver nanoparticles (AgNPs) is the most involved one in nano-medicine owing to their small size and large surface area [1]. Because of their established antimicrobial, antifungal and antiviral activities, they are growingly involved in multiple applications as food, consumer products, industrial and biomedical fields [2]. Concerns regarding potential toxicity and health risks are raised by their growing use. [3,4].

AgNPs accumulate principally in the liver [5] following inhalation [2], injections [6] and ingestion [7]. AgNPs build up excessively in the liver, causing a variety of pathological alterations, including inflammation, excess reactive oxygen species (ROS) production, DNA disruption, alteration in hepatic enzyme activities and ultimately necrotic and apoptotic changes [8]. AgNPs induce ROS production in different types of cells [9]. Both endogenous and exogenous antioxidants continuously produce and eliminate ROS in biological systems., yet their excess production leads to apoptosis and oxidative damage [10,11].

An antioxidant is a substance that directly scavenges ROS or indirectly acts to enhance antioxidant defenses or suppress ROS formation [12]. Many natural and synthetic antioxidants exist [13]. Silymarin (milk thistle) is a natural herbal medicine known for its therapeutic use in liver disorders due to its strong antioxidant and membrane-stabilizing functions [14]. As antioxidant, it reduces ROS and lipid peroxidation promoting hepatocyte regeneration, decreasing inflammatory reactions and inhibiting liver fibrogenesis induction [15]. Vitamin E is antioxidant and cyto-protective agent, which have been used for treating liver damage in viral infections, Amanita phalloides toxicity and cirrhosis because it can reduce oxidative stress by neutralizing ROS and reducing the oxidative stress cascade, reduce lipid peroxidation, stabilize mitochondrial membranes and prevent apoptotic cell death [16,17]. Both endogenous and exogenous antioxidants continuously produce and eliminate ROS in biological systems and have anti-inflammatory, platelet aggregation inhibition, signaling regulation, cellular proliferation, membrane-bound enzymes, and gene expression, and immune-enhancing properties in addition to its antioxidant activity [18,19]. A key regulator of normal cell physiology, mitochondrial

dynamics and calcium handling is the protein family of B cell lymphocyte-2 (BCL-2). It is located on outer membrane of mitochondrial and takes a major part in enhancing cell survival and suppressing pro-apoptotic proteins activity [20].

This study aim to explore AgNPs hepatotoxicity and the possible curative effects of mono- and combined Silymarin and Vitamin E therapy.

2. Material and methods

2.1. Material

2.1.a. Chemicals:

Silver nanoparticle (AgNPs): was purchased as clear colloidal aqueous suspension with a concentration of 4000PPM (4mg/L) and particles size 20-40NM (Nanotechnology and Biotechnology Lab, nanotechnology project, plant physiology department, Faculty of agriculture, Cairo university). Following a 30-day I.P of 0.5 mg AgNPs/kg B.W, the particles were diluted with distilled water (no color change or precipitation occurred), diluted with deionized water and sterilized with a 0.22 micron microfilter [21].

Silymarin: was provided as yellow fine powder (Sigma-Aldrich Chemical Company, USA) then dissolved in normal saline. A daily dosage of 100 mg/kg was administered for 30 successive days [22] orally by gastric gavage tube after 2 hours fasting; to avoid regurgitation and guarantee that the prescribed dosage was administered; the tube was remained in place for 20 seconds.

Vitamin E: was present in the form of yellow capsules, (each contains 400 mg), Pharco-Egypt. Each capsule was dissolved in 4ml/kg B.W. olive oil. It was administered orally in a dose of 400mg/kg B.W. [23] for 30 days by gastric gavage tube.

2.1.b. Animals: sixty four-month-old Sprague Dawley strain of male albino rats weighs 150–200g each. They were obtained from Faculty of Medicine's animal house-Cairo University, housed in cages with five rats each under standard lab and environmental conditions.

2.2. Study design:

The rats were divided into six groups:

- **Group I (Control-10 rats):** received no medications.
- **Group II (Sham control-10 rats):** this group was divided into two subgroups:

*** Subgroup II-A (Normal saline–5rats):** each rat was administered normal saline

orally using a gastric gavage tube every day for 30 successive days.

* **Subgroup II-B (Olive oil–5rats):** each rat was given 4ml/kg B.W. olive oil orally daily for 30 successive days.

- **Group III (AgNPs treated-10 rats):** each rat was injected I.P. with 0.5mg AgNPs/kg B.W. for 30 successive days.
- **Group IV (Silymarin treated–10 rats):** each rat was injected I.P. with 0.5mg AgNPs/kg B.W. for 30 successive days, then starting from the 31st day, each rat was given 100mg/kg silymarin orally daily for 30 successive days.
- **Group V (Vitamin E treated -10 rats):** each rat was injected I.P. with 0.5mg AgNPs/kg B.W. for 30 successive days, then, starting from the 31st day, each rat was given 400mg/kg B.W. vitamin E daily orally for 30 successive days.
- **Group VI (Silymarin and Vitamin E treated–10rats):** each rat was injected I.P. with 0.5mg AgNPs/kg B.W. for 30 successive ds, then, starting from the 31st day, each rat was given the calculated doses of Silymarin and vitamin E concomitantly orally for 30 successive days.

2.3. Methods:

By the end of designated experimental periods for each group, blood samples were collected from each rat's tail vein and sent for serum biochemical analysis for liver enzymes [24]. Then the rats were anesthetized with IP injection of 50mg/kg pentobarbital [25] and sacrificed. All groups' liver specimens underwent meticulous dissection and processing in preparation for:

a. Light microscopic study: preparation of liver specimen for light microscopic examination [26] then stained using:

-Hematoxylin and Eosin: to observe liver architecture [27].

-Masson's Trichrome stain: to evaluate fibrous tissue [28].

-Periodic acid-Schiff (PAS) staining: to identify liver glycogen storage [29].

-Immuno-histochemical staining for Bcl-2: avidin biotin peroxidase method was used in immunohisto-chemical procedures to determine Bcl-2 protein expression in the cytoplasm. (30).

-Histomorphometric analysis: making use of a Leica Qwin 500 Image Analyzer PC. Masson's Trichromes and immunohisto-chemically stained sections were morphometrically examined at Cairo

University's Pathology Department, Faculty of Dentists.

b. Serum biochemical analysis: utilizing commercial kits from Biodiagnostic Co. (Giza, Egypt) and an auto analyzer (Cobas INTEGRA 400 plus analyzer), aspartate aminotransferase (AST), Alkaline phosphatase (ALP) and alanine aminotransferase (ALT) levels [24,31] were measured at Cairo University's Faculty of Medicine's Biochemistry department.

c. Antioxidant biomarker and hepatic oxidative stress: malondialdehyde (MDA) [32] and glutathione (GSH) [33] content levels were determined in hepatic tissue according to by using commercial kit from Biodiagnostic (Giza, Egypt) were measured at Cairo University's Faculty of Medicine's Biochemistry department.

2.4. Statistical Analysis: one-way analysis of variance (ANOVA) was used to statistically analyze the collected data in order to compare the various groups. The least significant difference test (LSD), which determines the statistical difference between groups when an ANOVA is statistically significant (P value <0.05), comes next. The Statistical Package for the Social Sciences (SPSS) version 19 package was utilized for all statistical analyses.

3. Results:

3.1. Histological and immunohistochemicaL results:

- **Control groups (GI – GII): Light microscopic examination** revealed that there was no discernible difference between the normal and sham control groups' histology results. **H&E stained sections** of these groups showed normal architecture of hepatic parenchyma evidenced by peripherally located normal portal triad displayed normal thin walled portal vein, normal biliary ductules **(Figs. 1A,1B)** and normal thin walled central vein with uniform cords of hepatocytes radiating outwards from it. The hepatocytes appeared hexagonal in shape with regular outlines, granular acidophilic cytoplasm, darkly stained rounded vesicular nuclei and few binuclear hepatocytes **(Fig.1C)** with normal uniform thin walled hepatic sinusoids **(Figs.1B,1C)** in between. **PAS stained sections** exhibited a strong positive reaction in the form of small red granules filling the hepatocytes cytoplasm, implying the presence of significant amounts of

glycogen **(Fig.1D)**. **Masson's trichrome stained sections** demonstrated normal pattern of collagen fibers deposition around portal triads **(Fig.1E)**. **Immune-histochemical stained sections** revealed strong BCL-2 expression in liver cell cytoplasm **(Fig. 1F).**

- **AGNPs treated group (GIII):** all **H&E** stained sections revealed variable degrees of pathological changes distorting hepatic parenchymal architecture proved by spacing between the hepatocytes and around portal triad **(Fig. 2A)**, parenchyma and peri-portal inflammatory mononuclear cellular infiltration **(Fig.2B)**, focal areas of extracellular hemorrhage **(Fig.2C)**. Most of sections showed moderately dilated non-congested portal veins as well as mild biliary hyperplasia **(Fig.2A). PAS-stained specimens** showed mild reaction denoting diminished glycogen content within hepatocytes cytoplasm **(Fig. 2D)**. **Sections stained** with **Masson's trichrome** revealed marked peri-portal fibrosis **(Fig. 2E). Immuno-histochemical stained sections** revealed weak BCL-2 immune reaction with many negative cells **(Fig.2F).**

- **Silymarin monotherapy (GIV): H&E** stained specimens of this group partially regained the normal histological architecture. All specimens displayed few mildly dilated biliary ductules, minimally dilated congested portal veins as well as focal areas of peri-portal and parenchymal mononuclear cellular infiltration **(Fig.3A)**. Furthermore, there was mild dilatation of the congested hepatic sinusoids **(Figs. 3B)** with most of them showing Von Kupffer cells **(Figs. 3C)** in their walls. Most of the hepatocytes showed regular outlines, granular acidophilic cytoplasm with darkly stained rounded vesicular nuclei **(Figs. 3B, C)**; yet, others still showing karyolysis **(Fig. 3C).** No extra cellular hemorrhage detected in all specimens. **Sections stained** with **PAS** revealed positive reaction in some hepatocytes' cytoplasm **(Fig. 3D). Sections stained** A little number of collagen fibers surrounding the portal triad were seen using **Masson's trichrome (Fig. 3E). Immune-histochemical stained sections** revealed moderate positive BCL-2 expression **(Fig. 3F).**

- **Vitamin E monotherapy (GV)**: **H&E** sections of the rat liver tissue of this group demonstrated pathological changes less than that found in group III. Most of the specimen showed normally packed hepatocytes cords radiating from mildly

congested central vein. Normal peripherally located portal triad with normal portal vein and normal bile ductules **(Fig.4A).** All specimens showed no evidence of extra-cellular hemorrhage, yet localized peri-portal and parenchymal mononuclear cellular infiltrations and localized areas of spacing in between the hepatocytes **(Fig. 4C)** near the portal triad were noticed, mild to moderate dilatation and congestion of hepatic sinusoids **(Fig.4B)**. In few specimens, degenerated hepatocytes displayed ill-defined outlines, cytoplasmic rarefaction and nuclear pyknosis and karyolysis **(Fig.4C)**. **In PAS stained sections**, all hepatocytes displayed moderate positive reaction denoting moderate glycogen content **(Fig.4D). Masson's trichrome** displayed moderate fibrosis around portal triad **(Fig.4E). Sections stained** with **immunohistochemistry** showed a moderate BCL-2 expression in hepatocytes cytoplasm **(Fig.4F).**

- **Combined Silymarin and Vitamin E therapy (GVI)**: **H&E stained sections** showed near normal hepatic architecture as compared to groups IV and V. Almost all central and portal veins appeared normal, apart from few mildly dilated and congested ones, localized peri-portal mononuclear cellular infiltrations and normal biliary ductules **(Fig. 5A)**. Few hepatic sinusoids displayed mild dilatation with some of them appeared minimally congested and others were non-congested **(Figs.5B)** with few Von Kupffer cells seen **(Fig.5C)** within. Most of the hepatocytes showed granular acidophilic cytoplasm with darkly stained rounded vesicular nuclei, while few still displaying karyolysis and pyknosis of their nuclei **(Fig.5C)**. No extracellular hemorrhage detected in all examined specimens. **PAS stain** elicited moderate staining of hepatocyte cytoplasm denoting high glycogen content **(Fig.5D**). **Sections stained** with **Masson's trichrome** revealed mild peri-portal collagen fibers deposition **(Fig.5E). Immune-histochemical stained sections** demonstrated intense cytoplasmic expression of BCL- 2 **(Fig.5F)**.

3.2. Biochemical and statistical results:

-As shown in **Figs. 6A, 6B, 6C, ALT, AST and ALP** serum levels showed no statistical significant difference between control groups (GI- GII), while, their mean values in the AgNPs-treated group (GIII) increased statistically significant (p <

0.001) in comparison to control groups. Silymarin and Vitamin E therapeutic groups (GIV, GV, GVI) showed statistical significant reduction of hepatic enzymes serum levels as compared to GIII, with near normal result recorded combined therapy in GVI. Although, The AST levels of GIV and GV did not show statistically significant difference, yet they were statistically significant higher than the control groups.

-The oxidative stress **MDA** radicle and antioxidant **GSH** levels in AgNPs treated rats showed dramatic rise in MDA and decline in GSH levels in contrast to the control groups. On the contrary, significant statistical lowering in MDA and elevation of GSH activities was detected in Silymarin and vitamin E treated groups as compared to group III, being remarkable in combined anti-oxidant treatment in GVI **(Figs. 6D, 6E).**

3.3. Histomorphometric findings:

The mean% area of collagen fibers and mean values of BCL-2 optical density revealed no statistical difference between the control groups. High statistical significant increase in peri-portal collagen fibers deposition and decline in Bcl-2 expression were found in GIII as compared to control groups, IV, V and VI indicating AgNPs hepatotoxicity with increased cellular apoptosis. In contrast, groups IV, IV and V showed noticeable decline in peri-portal fibrosis and increase in BCL2 expression as compared to GIII indicating recovery with the best results documented in GVI. Interestingly, Vitamin E single therapy showed higher increase in peri-portal fibrosis as compared to Silymarin single and combined therapy indicating that Silymarin has higher potentials in reducing hepatic fibrosis more than vitamin E **(Figs. 7A, 7B).**

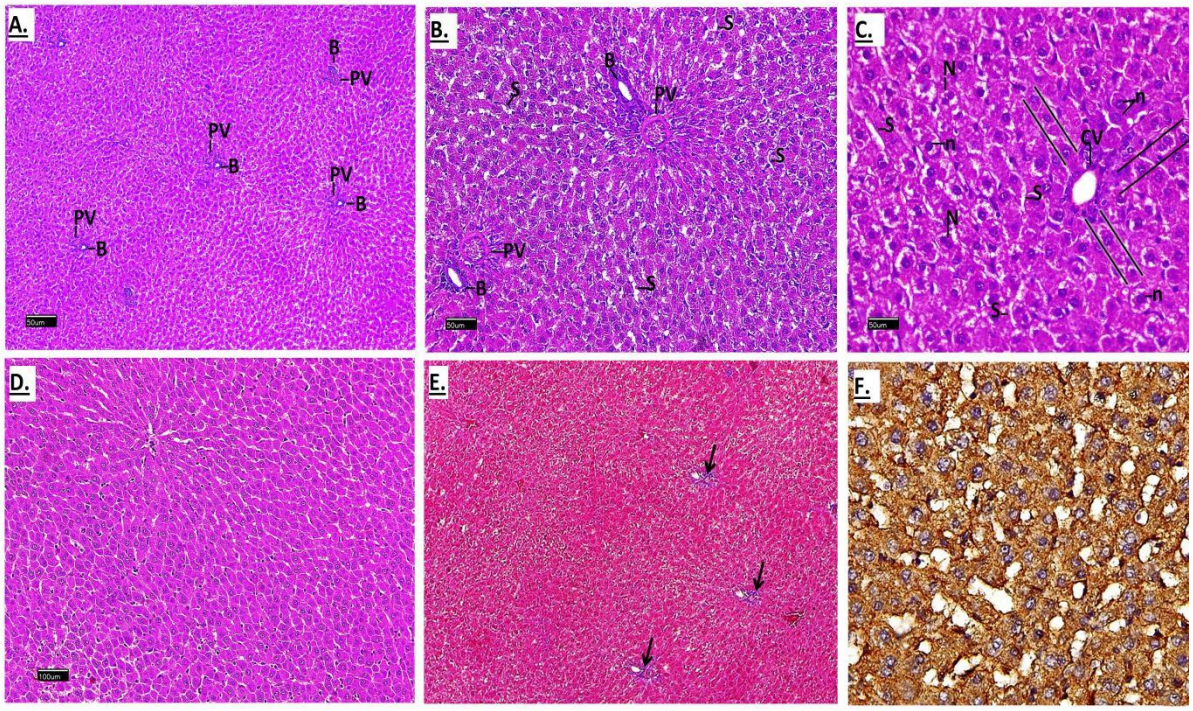

Figure (1): Photomicrographs of rat liver tissue of the control groups. **A.** showing normal hepatic parenchyma with normal thin walled portal veins (PV) and normal biliary ductules (B) **(H&E X100). B.** showing normal hepatic parenchyma displaying normal thin walled portal veins (PV), normal biliary ductules (B) and uniform hepatic sinusoids (S) between the hepatocytes**(H&E X200). C.** showing normal hexagonal hepatocytes radiating (bracketed by lines) from the normal thin wall central vein (CV) and uniform thin wall hepatic sinusoids (S) seen between the hepatocytes. All hepatocytes show regular outlines, granular acidophilic cytoplasm with darkly stained rounded vesicular nuclei (n) with few binuclear hepatocytes (N) **(H&EX400). D.** showing strong positive PAS reaction within the cytoplasm of hepatocytes **(PASX200). E.** showing normal pattern of collagen fiber deposition (arrows) around portal triads **(M.T. X100). F.** revealed strong BCL-2 reaction with positive cells **(BCL-2 X400).**

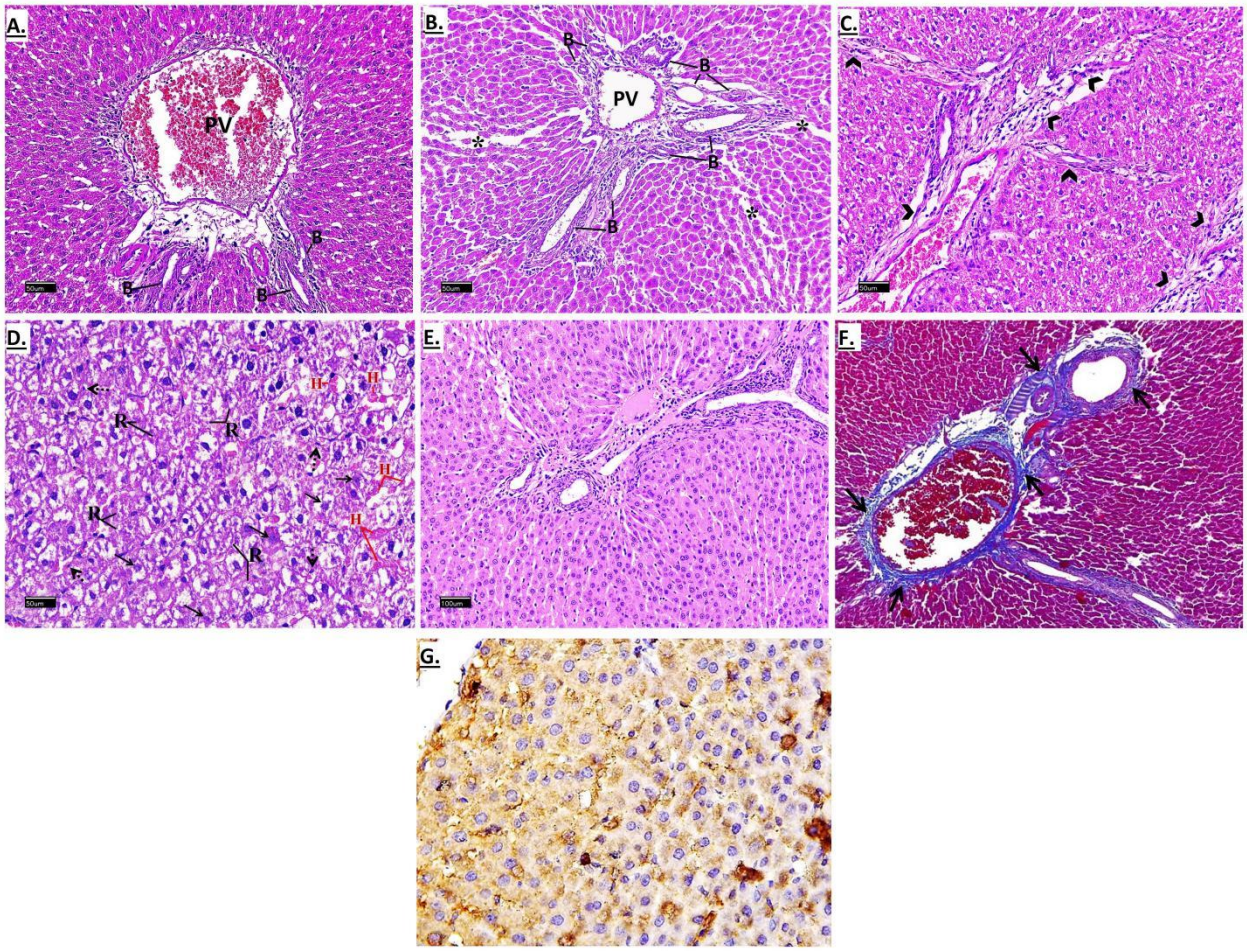

Figure (2): Photomicrographs of rat liver tissue of group III. **A.** showing thin irregular walled markedly dilated congested portal vein (PV) surrounded by mild biliary ductules hyperplasia (C). **B.** showing moderately dilated thin walled non congested portal vein (PV) surrounded by mild biliary ductules hyperplasia (B) as well as spacing between the hepatocytes (*) **(H&E X100). C.** showing wide areas of mononuclear infiltration (arrowheads) surrounding the portal triad and extends through the hepatic parenchyma **(H&E X200). D.** showing distorted hepatic parenchymal architecture. The hepatocytes show degenerative changes in the form of cytoplasmic rarefaction (R), pyknosis (dotted arrows) and karyolysis (thin arrows) of the nuclei. Focal areas of extracellular hemorrhage (H) are also noted **(H&E X400). E.** showing mild PAS reaction within the cytoplasm of hepatocytes **(PAS X200). F.** showing marked increase in collagen fibers (arrows) deposition around the portal triad **(M.T. X100). G.** revealed weak BCL-2 reaction with many negative cells **(BCL-2 X400).**

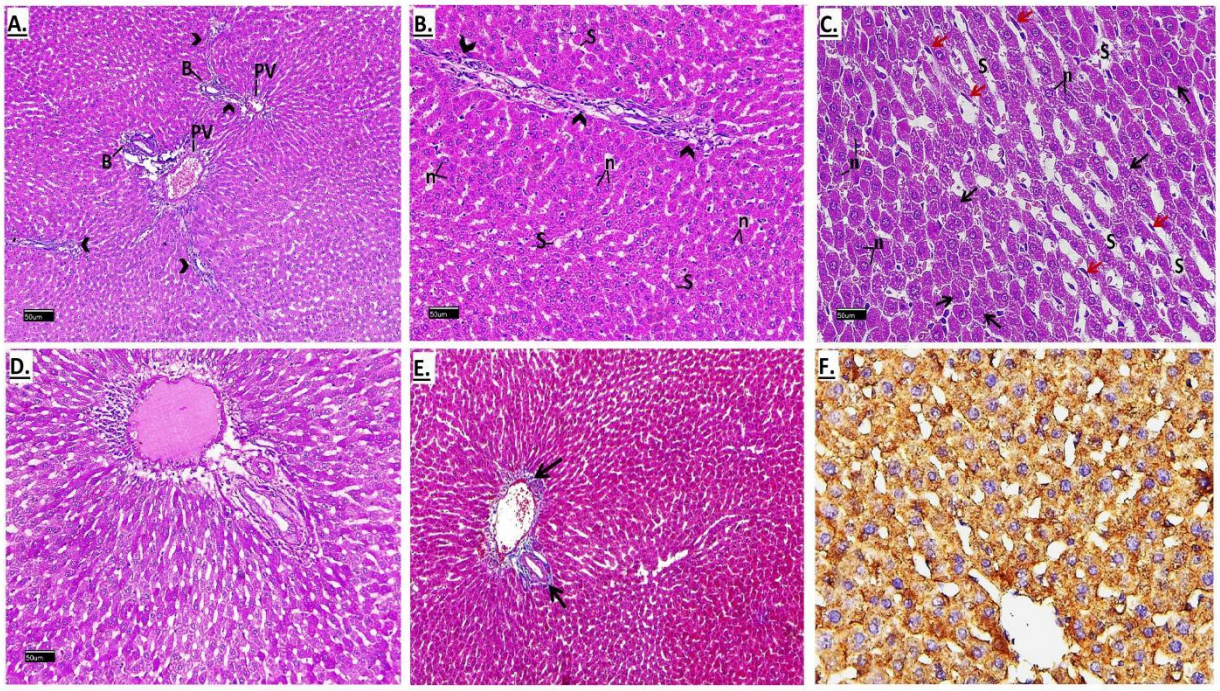

Figure (3): Photomicrographs of rat liver tissue of group IV. **A.** showing partial restoration of normal hepatic parenchymal architecture in the form of variable degree of mildly dilated, congestion portal veins (PV) and few mildly dilated biliary ductules (B). Focal areas of peri-portal mononuclear infiltration (arrowheads) are seen around the portal triad and traversing the hepatic parenchyma **(H&E X100). B.** showing focal parenchymal mononuclear cellular infiltration (arrowheads) and mild dilatation and congestion of hepatic sinusoids (S). Most of the hepatocytes show normal rounded darkly stained vesicular nuclei (n) **(H&E X200). C.** showing mildly dilated, mildly congested hepatic sinusoids (S) with multiple Von Kupffer cells (red arrows). Most of the hepatocytes show regular outlines, granular acidophilic cytoplasm with darkly stained rounded vesicular nuclei (n) a part from few showing karyolysis (thin arrow) of their nuclei **(H&E X400). D.** showing moderate positive PAS reaction in the cytoplasm of some hepatocytes **(PAS X200). E.** showing mild amount of collagen fibers (arrows) encircling the portal triad **(M.T. X100). F.** revealed moderate positive BCL-2 reaction within the cytoplasm of hepatocytes **(BCL-2 X400).**

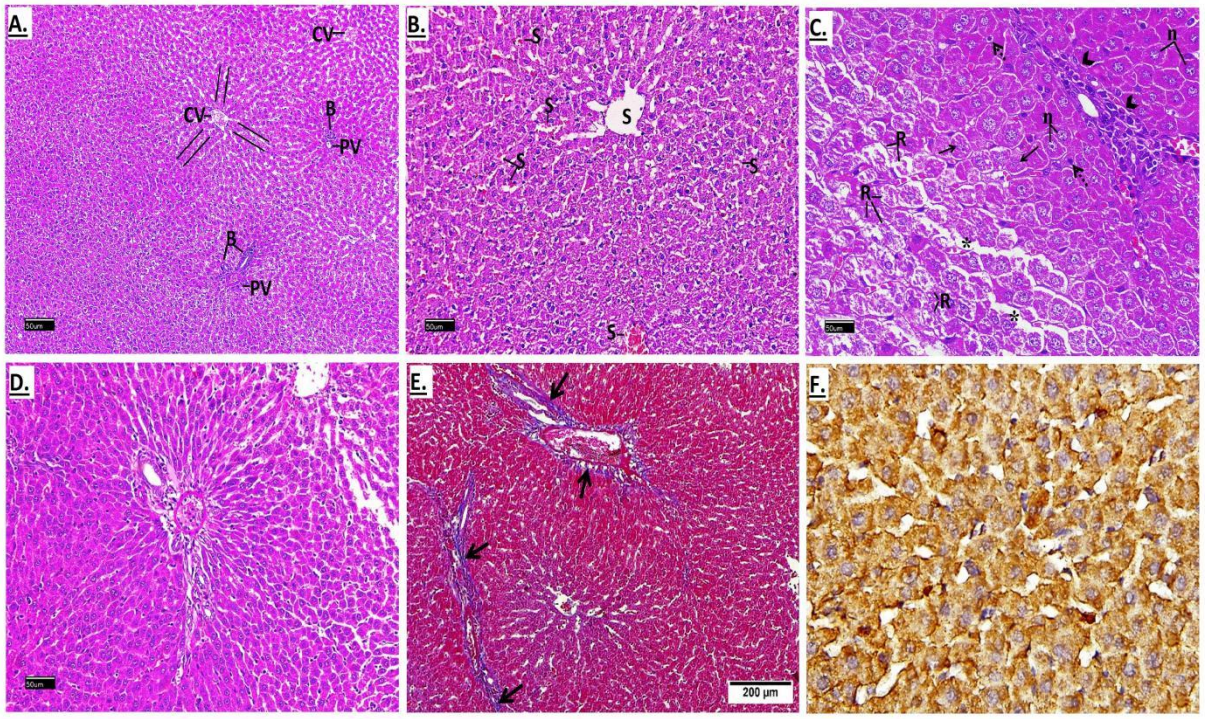

Figure. (4): Photomicrographs of rat liver tissue of group V. **A.** showing preserved hepatic parenchymal architecture with normally packed radiating hepatocytes cords (bracketed by lines) from mildly congested central veins (CV) with normal portal vein (PV) and normal biliary ductules (B) **(H&E X100) . B.** showing mild to moderate dilatation and congestion of hepatic sinusoids (S) **(H&E X200). C.** showing localized area of hepatic parenchymal architecture distortion in the form of spacing (*) between the hepatocytes. Some hepatocytes show degenerative changes in the form of ill-defined outlines, cytoplasmic rarefaction (R), karyolysis (thin arrows) and pyknosis (dotted arrows) of their nuclei. Few hepatocytes show normal granular acidophilic cytoplasm with darkly stained rounded vesicular nuclei (n). Focal parenchymal area of mononuclear infiltration (arrowheads) is also noted **(H&E X400). D.** showing moderate positive PAS reaction in the cytoplasm of all hepatocytes **(PAS X200). E.** showing moderate amount of collagen fibers (arrows) encircling the portal triad **(M.T. X100). F.** revealed moderate positive BCL-2 reaction within the cytoplasm of hepatocytes **(BCL-2 X400).**

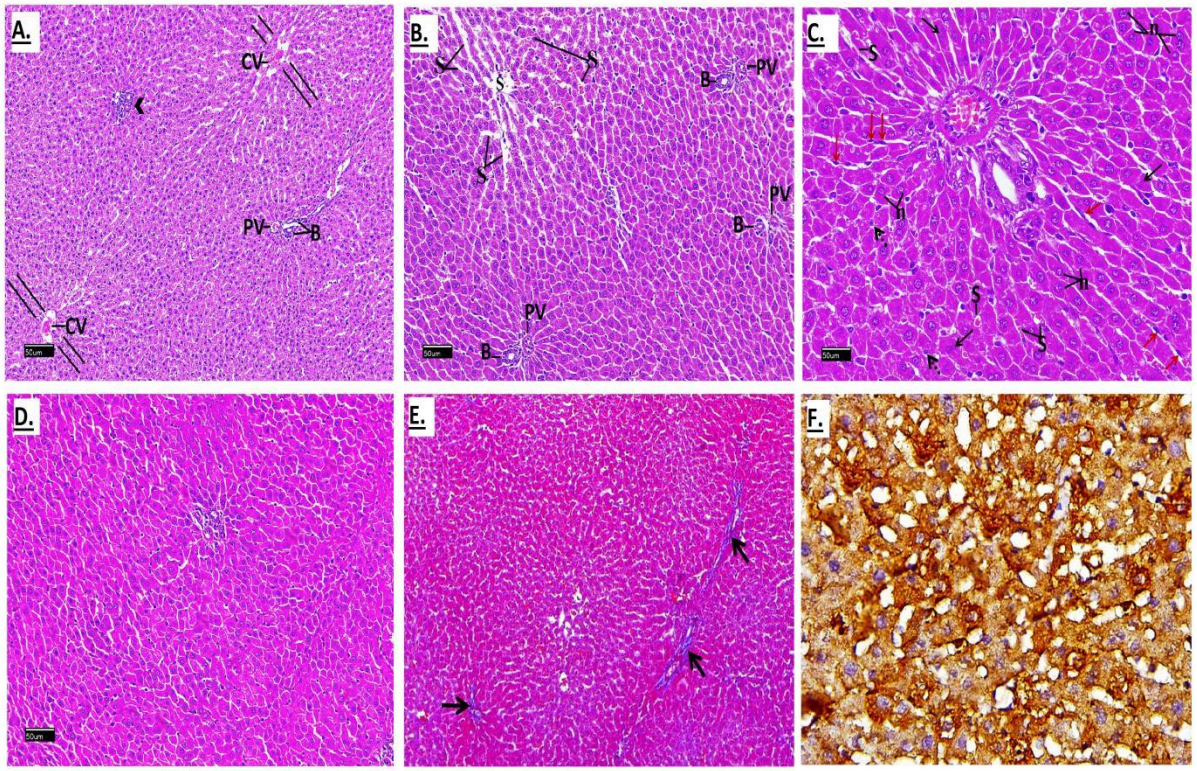

Figure. (5): Photomicrographs of rat liver tissue of group VI. **A.** showing radiating hepatic cords (bracketed by lines) from mildly dilated congested central veins (CV) with minimally dilated portal veins (PV) and normal biliary ductules (B). Scanty mononuclear infiltration (arrowhead) is seen surrounding the portal triad **(H&E X100). B.** showing mildly dilated congested and non-congested hepatic sinusoids (S). Preserved portal triad displaying normal portal vein (PV) and normal biliary ductules (B) **(H&E X200). C.** showing minimally congested hepatic sinusoids (S) with few Von Kupffer cells (red arrows) seen within. Most of the hepatocytes show granular acidophilic cytoplasm with darkly stained rounded vesicular nuclei (n) with few showing karyolysis (thin arrows) and pyknosis (dotted arrows) of their nuclei **(H&E X400). D.** showing moderate positive PAS reaction in the cytoplasm of all hepatocytes **(PAS X200). E.** showing mild amount of collagen fibers (arrows) encircling the portal triad **(MT. X100). F.** revealed strong positive BCL-2 reaction within the cytoplasm of hepatocytes **(BCL-2 X400).**

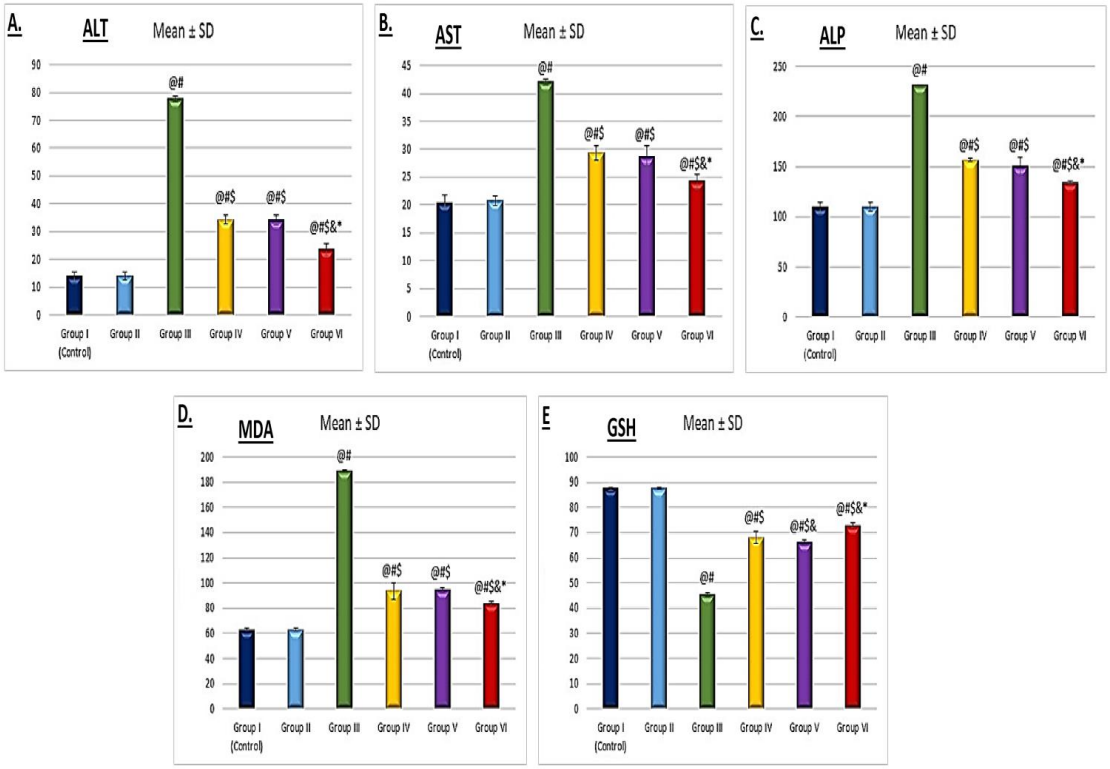

Figure (6): Bar charts showing comparison between **ALT, AST, ALP, MDA and GSH** levels in different groups: @ Significant from control, # significant from group II, $ significant from group III, & significant from group IV, * significant from group V.

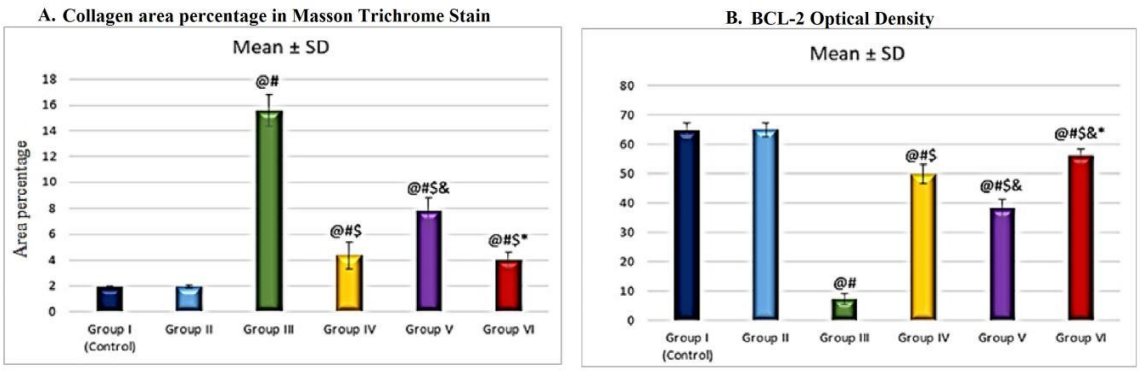

Figure (7): **A.** Bar charts showing comparison between **collagen area percentage in Masson Trichrome Stain** levels, **B.** Bar chart showing comparison between **optical density of the Bcl-2 expression** levels in different groups @ significant from control, # significant from group II, $ significant from group III, & significant from group IV, * significant from group

4. Discussion:

AgNPs are the utmost utilized metallic nanoparticles. They are involved in managing several diseases such as liver injury [34,35,36], cardiac injury [37], pulmonary inflammation [38] and anti-neoplastic agent [39]. Despite the fact that oxidative stress, DNA damage, cytotoxicity, and inflammatory reactions were noted [40], yet the exact mechanism of toxicity is still a mystery [41]. ROS over-production is greatly incriminated in AgNPs cytotoxicity [42, 43,44].

Hassan et al. (2019) reported that the liver is where AgNPs primarily accumulate, followed by the kidneys, spleen, and lungs. **Chalasani et al. (2015)** elucidated that AgNps accumulate in the liver with consequent aggregates formation, result in mechanical cellular damage and functional disturbance. Further studies linked AgNps toxicity to their shape, size, coating and surface electric charge with the small positively charged ones being more destructive [47]. **Ferdous and Nemmar (2020)** proved that the extent of hepatotoxicity is proportionate to the size, dose and duration of AgNPs administration. In the present work, hepatic toxicity was generated by injecting 0.5mg /kg AgNPs I.P. for 30days, which was in agreement with **Bastús et al. (2014)**. AgNPs treated rats led to disrupted hepatic architecture, dilated congested central and portal veins and significant hepatic sinusoids dilatation. That was in agreement with **Assar et al. (2022)** who added that reduction in liver weight was the first symptom and could be attributed to accelerated lipid peroxidation.

The current result illustrated diffuse mild biliary hyperplasia with few markedly dilated ones. That was in partial consciences with **Blanco et al. (2018)**, who reported that after receiving daily intraperitoneal injections of AgNps at varying doses for 28 days, the most frequent outcome was cholangiopathy (1, 2, 4mg/kg B.W). In each treatment group, it was found to be dose dependent.

However, **Moradi-Sardareh et al. (2018)** showed that after 9 days of intraperitoneal injection, different AgNPs (0.25, 0.5, 1mg/kg) dosages were unable to produce any appreciable histological alterations. They suggested that their findings might be the consequence of the brief administration duration.

The conducted work displayed hepatocytes cytoplasmic vacuolation/rarefaction, nuclear pyknosis and/or karyolysis as well as focal areas of extracellular hemorrhage. Similar results were reported following I.P injection of very high doses (25, 100 mg/kg) of AgNPs for 14 days [51]. In the present study, peri-portal and parenchymal inflammatory cellular infiltration was elucidated, which was in keeping with **Jia and colleagues (2013)** who demonstrated that silver nano enhances the pro-inflammatory activity of kupffer cells leading to inflammatory changes and reduces fatty acid oxidation.

Silymarin therapy in GIV partially alleviated AgNPs induced liver injury, which was in agreement with **Bayader et al. (2013)**. Although, it can attenuate inflammatory cascades, oxidative stress and fibrotic changes, its precise mechanism of action is

still unrevealed [54]. In GV, giving 400mg/kg Vitamin E orally for 30 ds exhibited hepato-protective effects, which was in accordance to **Kuribayashi et al. (2010)**. On the contrary, **Bashandy (2006)** demonstrated that giving 100mg/kg Vitamin E daily for 28 ds was able to counteract hepatic damage following lead toxicity. Vitamin E treated rats showed partial restoration of histological structure, which were in agreement with trials carried out by **Phung et al. (2009)**, using non-alcoholic fatty liver rat model and **Karimian et al. (2015)** using mouse model following partial hepatectomy. Moreover, recent studies proved that 100mg/kg vitamin E amended AgNPs toxicity in tongue papillae [58] and submandibular salivary glands]59].

Combined Vitamin E and Silymarin therapy showed almost normal hepatic architecture as compared to single Vitamin E or Silymarin treatment. Parallel to these results, **Lamia and colleagues (2021)** demonstrated that Silymarin (140mg/kg/day) therapeutic effects were boosted by coenzyme Q10 (200 mg/kg/day) when given for 4weeks versus carbon tetrachloride inflected liver damage in an ovariectomized female rat model. Likewise, coupled vitamin E and C treatment against AgNPs accumulation in both liver and kidneys was more effective than giving each drug along [61].

PAS-stained samples clarified normal hepatic glycogen content in control groups, which was markedly diminished after AgNPs injection. Silymarin and Vitamin E single or combined therapy partially replenished hepatic glycogen store, with the best result achieved by anti-oxidant co-treatment. Comparable results recorded by **Abo-El-Sooud et al. (2023)** who stated that daily garlic acid (20 mg/k) treatment significantly regained hepatocytes glycogen content after sub-chronic Zinc oxide nanoparticles (100 mg ZNPs/kg) treatment. Masson's trichrome histological sections and histomorphometric data, illustrated marked peri-portal tract fibrosis with high statistical significant ($p<0.001$) in GIII, which was declined after Silymarin therapy more than Vitamin E single administration with the best results obtained on giving both. These results were in accordance with **Assar et al. (2022)**, who found marked thickening of hepatic capsule and increase in inter- and intra-lobular fibrosis. In contrast, **Yousof et al. (2022)** recorded no abnormal collagen deposition on giving 0.5ml AgNPs (of a solution with 25 ppm AgNPs) orally for 14days.

In the current work, AgNPs-mediated apoptotic cell death is indicated by significant reduction ($p<0.001$) in Bcl-2 immune expression. Treatment with Silymarin and vitamin E showed moderate Bcl-2 immune expression, which was augmented by their concomitant administration in GVI. **Zielinska et al. (2018)** recorded similar findings.

The histological and immunohisto-chemical results were emphasized by biochemical findings. Rats given AgNPs displayed a statistically significant ($p<0.001$) rise in liver enzymes. Monotherapy with Silymarin or Vitamin E relatively lowered liver enzymes levels, with near normal result following their combined administration. Lately, liver damage and raised liver

enzymes following short [65] and long [48] exposure to AgNps were observed, which was in partial agreement to the present work. In contrast, **Yousof and co-workers (2022)** recorded no statistical difference in ALT and AST levels between AgNPs treated mice for two distinct periods (14 and 28 days) and the control ones.

MDA is the principle oxidative stress marker [66]. GSH is an antioxidant scavenger that was implicated in the pathogenesis of multiple disorders [67]. In the current work, hepatic MDA levels is significant increased and is accompanied by significant depletion of GSH in GIII ($p<0.001$), which proved that AgNPs-induced hepatotoxicity is mediated via enhancing oxidative stress and lipid peroxidation with reduction in antioxidant activity. Single administration of Silymarin or vitamin E partially alleviated oxidative stress and enhanced antioxidant activities as compared with GIII ($p < 0.001$) with almost normal results found after combination antioxidant therapy in GVI. Many studies were in keeping with the current findings **(60,68)**. **Atiba et al. (2016)** postulate that AgNPs have great affinity for thiol group with consequent reaction with the sulfur containing proteins such as GSH, leading to GSH depletion.

5. Conclusion

The current study confirmed the hepatotoxic effect of AgNPs histologically, immunohistochemically and biochemically, which is probably carried out via enhancing inflammation, lipid peroxidation, enzymatic impairment, excess ROS formation with consequent oxidative stress damage and eventually apoptotic cell death. Mono-therapy with antioxidants Silymarin or Vitamin E succeeded to partially alleviate AgNPs induced toxicity. Interestingly, Silymarin displayed higher potentials in reducing peri-portal fibrosis more than vitamin E. while, near normal result achieved by co-treatment with Silymarin and Vitamin E.

Acknowledgment

Ethical approval and consent to: the research was approved by the university scientific research ethics committee for experimental animals at Faculty of Medicine, Fayoum University at 12/4/2023 number (M 649). All animals' experimental procedures were done according to the approved standards for care and use of laboratory animals.

Participate:

Funding: There is no funding for this study.

Conflicts of Interest: No conflicts of interest are disclosed by any of the authors.

References:

1. Zhang XF, Liu ZG, Shen W, Gurunathan S. Silver nanoparticles: synthesis, characterization, properties, applications, and therapeutic approaches. International journal of molecular sciences.2016;17(9):1534.doi.org/10.3390/ijms17091534.
2. Gurunathan S, Park JH, Han JW, Kim JH. Comparative Assessment of the Apoptotic Potential of Silver Nanoparticles Synthesized by Bacillus Tequilensis and Calocybe Indica in MDA-MB-231 Human Breast Cancer Cells: Targeting p53 for Anticancer Therapy [Corrigendum]. International Journal of Nanomedicine.2022;17:5207-8. doi.org/10.2147/IJN.S395879
3. Yarmohammadi P, Arabi M, Yarmohammadi P. Subacute dermal toxicity investigation of nanosilver on serum chemical biomarkers in male mice. Nanomed J. 2014 ;1(4):285-91.doi.org/10.7508/nmj.2015.04.009
4. Theodorou IG, Ryan MP, Tetley TD, Porter AE. Inhalation of silver nanomaterials—Seeing the risks. International journal of molecular sciences.2014;15(12):23936-74. doi.org/10.3390/ijms151223936
5. De Jong WH, Van Der Ven LT, Sleijffers A, Park MV, Jansen EH, Van Loveren H, Vandebriel RJ. Systemic and immunotoxicity of silver nanoparticles in an intravenous 28 days repeated dose toxicity study in rats. Biomaterials. 2013;34(33):833343.doi.org/10.1016/j.biomaterials.2013.06.048.
6. Hirn S, Semmler-Behnke M, Schleh C, Wenk A, Lipka J, Schäffler M, Takenaka S, Möller W, Schmid G, Simon U, Kreyling WG. Particle size-dependent and surface charge-dependent biodistribution of gold nanoparticles after intravenous administration. European journal of pharmaceutics and biopharmaceutics. 2011;77(3):407-16.doi.org/10.1016/j.ejpb.2010.12.029
7. Schleh C, Semmler-Behnke M,Lipka J, Wenk A, Hirn S, Schäffler M, Schmid G, Simon U, Kreyling WG. Size and surface charge of gold nanoparticles determine absorption across intestinal barriers and accumulation in secondary target organs after oral administration. Nanotoxicology.2012;6(1):36-46. doi.org/10.3109/17435390.2011.552811
8. Lee WM. Drug-induced acute liver failure. Clinics in liver disease. 2013 ;17(4):75-86. doi.org/10.1016/j.cld.2013.07.001.
9. Choi O, Clevenger TE, Deng B, Surampalli RY, Ross Jr L, Hu Z. Role of sulfide and ligand strength in controlling nanosilver toxicity. Water research. 2009;43(7):1879-86. doi.org/10.1016/j.watres.2009.01.029.
10. Piao MJ, Kang KA, Lee IK, Kim HS, Kim S, Choi JY, Choi J, Hyun JW. Silver nanoparticles induce oxidative cell damage in human liver cells through inhibition of reduced glutathione and induction of mitochondria-involved apoptosis. Toxicology letters. 2011;201(1):92-100. doi.org/10.1016/j.toxlet.2010.12.010
11. Xu Y, Ayrapetov MK, Xu C, Gursoy-Yuzugullu O, Hu Y, Price BD. Histone H2A. Z controls a critical chromatin remodeling step required for DNA double-strand break repair. Molecular cell. 2012;48(5):723-33.doi: 10.1016/j.molcel.2012.09.026
12. Gulcin İ. Antioxidants and antioxidant methods: an updated overview. Arch Toxicology. 2020;94(3):651-715. doi: 10.1007/s00204-020-02689-3.
13. Neha K, Haider MR, Pathak A, Yar MS. Medicinal prospects of antioxidants: A review. Eur J Med Chem. 2019; 15; 178:687-704.doi: 10.1016/j.ejmech.2019.06.010.
14. Gillessen A , Schmidt HHJ. Silymarin as Supportive Treatment in Liver Diseases: A Narrative Review. Advances in Therapy.2020; 37(4), 1279–1301. doi: 10.1007/s12325-020-01251-y.
15. Fehér J, Lengyel G. Silymarin in the prevention and treatment of liver diseases and primary liver cancer. Current pharmaceutical biotechnology. 2012; 13(1):210-7.
16. https://doi.org/10.2174/138920112798868818
17. Liu Z, Ren Z, Zhang J, Chuang CC, Kandaswamy E, Zhou T, Zuo L. Role of ROS and nutritional antioxidants in human diseases. Frontiers in physiology. 2018 ;9:360203.doi.org/10.3389/fphys.2018.00477
18. Jamali B, Entezari M, Babaei N, Hashemi M. The evaluation of vitamin E and TiO2 nanoparticles administration in parkinson's rat model. Cell Journal (Yakhteh).2023;25(2):102. doi: 10.22074/cellj.2022.557558.1071
19. Rizvi S, Raza ST, Ahmed F, Ahmad A, Abbas S, Mahdi F. The role of vitamin e in human health and some diseases. Sultan Qaboos Univ Med J. 2014;14(2):e157-65.

20. Hadi HE, Vettor R, Rossato M. Vitamin E as a treatment for nonalcoholic fatty liver disease: reality or myth?. Antioxidants. 2018 ;7(1):12. doi.org/10.3390/antiox7010012
21. Zhang J, Wang F, Yalamarty SSK, Filipczak N, Jin Y, Li X. Nano Silver-Induced Toxicity and Associated Mechanisms. Int J Nanomedicine. 2022;17:1851-1864. doi: 10.2147/IJN.S355131.
22. Bastús NG, Merkoçi F, Piella J, Puntes V. Synthesis of highly monodisperse citrate-stabilized silver nanoparticles of up to 200 nm: kinetic control and catalytic properties. Chemistry of Materials. 2014;26(9):2836-46. doi.org/10.1021/cm500316k
23. Taleb A, Ahmad KA, Ihsan AU, Qu J, Lin NA, Hezam K, Koju N, Hui L, Qilong D. Antioxidant effects and mechanism of silymarin in oxidative stress induced cardiovascular diseases. Biomedicine & Pharmacotherapy. 2018;102:689-98. doi.org/10.1016/j.biopha.2018.03.140
24. Kuribayashi M, Fujioka M, Takahashi KA, Arai Y, Ishida M, Goto T, Kubo T. Vitamin E prevents steroid-induced osteonecrosis in rabbits. Acta orthopaedica. 2010;81(1):154-60. doi.org/10.3109/17453671003628772
25. Latimer KS. Duncan & Prasse's Veterinary Laboratory Medicine : Clinical Pathology. 5th ed. Wiley-Blackwell; 2011.
26. Bennett K, Lewis K. Sedation and Anesthesia in Rodents. Vet Clin North Am Exot Anim Pract. 2022 ;25(1):211-255. doi: 10.1016/j.cvex.2021.08.013.
27. Suvarna KS, Layton C, Bancroft JD. Bancroft's theory and practice of histological techniques.8th ed. Elsevier health sciences; 2018 .
28. Llewellyn BD. Nuclear staining with alum hematoxylin. Biotechnic & Histochemistry. 2009;84(4):159-177.doi.org/10.1080/10520290903052899
29. Bancroft JD, Gamble M. Theory and practice of Histological Techniques. Elsevier health sciences. 6th ed, Churchill Livingstone, Elsevier, China;2008.
30. Ross MH , Pawlina W. Histology. A Text and Atlas with correlated cell and molecular biology. 6th edition. Pb. Lippincott Williams and Wilkins; 2011. P: 628-636.
31. Kiernan JA. Histological and Histochemical Methods: Theory and Practice.5th edition. Scion Publishing, Folia histochemica et cytobiologica.;2015. 571 pp.
32. Schumann G, Klauke R, Canalias F, Bossert-Reuther S, FH Franck P, Gella FJ, J. Jørgensen P, Kang D, Lessinger JM, Panteghini M, Ceriotti F. IFCC primary reference procedures for the measurement of catalytic activity concentrations of enzymes at 37 C. Part 9: Reference procedure for the measurement of catalytic concentration of alkaline phosphatase: International Federation of Clinical Chemistry and Laboratory Medicine (IFCC) Scientific Division, Committee on Reference Systems of Enzymes (C-RSE) 1. Clinical chemistry and laboratory medicine. 2011;49(9):1439-46. doi.org/10.1515/CCLM.2011.621
33. Buege JA, Aust SD. Microsomal lipid peroxidation. Methods Enzymol. 1978;52:302-10. doi: 10.1016/s0076-6879(78)52032-6.
34. Moron MS, Depierre JW, Mannervik B. Levels of glutathione, glutathione reductase and glutathione S-transferase activities in rat lung and liver. Biochim Biophys Acta. 1979 Jan 4;582(1):67-78. doi: 10.1016/0304-4165(79)90289-7.
35. Lee SH, Jun BH. Silver nanoparticles: synthesis and application for nanomedicine. International journal of molecular sciences. 2019 ;20(4):865.doi.org/10.3390/ijms20040865
36. Alajmi RA, Al-Megrin WA, Metwally D, Al-Subaie H, Altamrah N, Barakat AM, Abdel Moneim AE, Al-Otaibi TT, El-Khadragy M. Anti-Toxoplasma activity of silver nanoparticles green synthesized with Phoenix dactylifera and Ziziphus spina-christi extracts which inhibits inflammation through liver regulation of cytokines in Balb/c mice. Bioscience reports. 2019;39(5):BSR20190379. doi.org/10.1042/BSR20190379
37. Arozal W, Monayo ER, Barinda AJ, Perkasa DP, Soetikno V, Nafrialdi N, Louisa M. Protective effects of silver nanoparticles in isoproterenol-induced myocardial infarction in rats. Frontiers in Medicine.2022;9:867497. doi.org/10.3389/fmed.2022.867497
38. Alharbi HY, Helmi NW, Salem NA. Possible Protective Effect of Silver Nanoparticles against Cisplatin Induced Pulmonary Inflammation in Rat Model. J. Pharm. Res. Int. 2021 :453-63. doi:10.9734/JPRI/2021/v33i46A32888
39. Prasannaraj G, Venkatachalam P. Hepatoprotective effect of engineered silver nanoparticles coated bioactive compounds against diethylnitrosamine induced hepatocarcinogenesis in experimental mice.

Journal of Photochemistry and Photobiology B: Biology. 2017 ;167:309-20. doi.org/10.1016/j.jphotobiol.2017.01.009

40. Akter M, Sikder MT, Rahman MM, Ullah AA, Hossain KF, Banik S, Hosokawa T, Saito T, Kurasaki M. A systematic review on silver nanoparticles-induced cytotoxicity: Physicochemical properties and perspectives. Journal of advanced research. 2018 ;9:1-6. doi.org/10.1016/j.jare.2017.10.008
41. Olugbodi JO, Lawal B, Bako G, Onikanni AS, Abolenin SM, Mohammud SS, Ataya FS, Batiha GE. Effect of sub-dermal exposure of silver nanoparticles on hepatic, renal and cardiac functions accompanying oxidative damage in male Wistar rats. Scientific Reports. 2023 ;13(1):10539. doi: 10.1038/s41598-023-37178-x.
42. Barcińska E, Wierzbicka J, Zauszkiewicz-Pawlak A, Jacewicz D, Dabrowska A, Inkielewicz-Stepniak I. Role of Oxidative and Nitro-Oxidative Damage in Silver Nanoparticles Cytotoxic Effect against Human Pancreatic Ductal Adenocarcinoma Cells. Oxidative Medicine and Cellular Longevity.2018;(1):8251961. doi.org/10.1155/2018/8251961
43. Morais M, Teixeira AL, Dias F, Machado V, Medeiros R, Prior JA. Cytotoxic effect of silver nanoparticles synthesized by green methods in cancer. Journal of Medicinal Chemistry.2020;63(23):1430835.doi.org/10.1021/acs.jmedchem.0c01055
44. Bandyopadhyay A, Roy B, Shaw P, Mondal P, Mondal MK, Chowdhury P, Bhattacharya S, Chattopadhyay A. Cytotoxic effect of green synthesized silver nanoparticles in MCF7 and MDA-MB-231 human breast cancer cells in vitro. The Nucleus. 2019;63(2):191-202.doi:10.1007/s13237-019-00325-z.
45. Jaswal T, Gupta J. A review on the toxicity of silver nanoparticles on human health. Materials Today: Proceedings. 2023;81:859-63. doi.org/10.1016/j.matpr.2021.04.266
46. Hassan OA, Saad AH, Hamouda AH. Silver nanoparticles induced multiple organ toxicity in mice. The Egyptian Journal of Forensic Sciences and Applied Toxicology. 2019;19(4):31-47. doi.10.21608/ejfsat.2019.12218.1070
47. Chalasani N, Bonkovsky HL, Fontana R, Lee W, Stolz A, Talwalkar J, Reddy KR, Watkins PB, Navarro V, Barnhart H, Gu J. Features and outcomes of 899 patients with drug-induced liver injury: the DILIN prospective study. Gastroenterology.2015;148(7):1340-52. doi.org/10.1053/j.gastro.2015.03.006
48. Ferdous Z, Nemmar A. Health impact of silver nanoparticles: a review of the biodistribution and toxicity following various routes of exposure. International journal of molecular sciences. 2020 ;21(7):2375.doi.org/10.3390/ijms21072375
49. Assar DH, Mokhbatly AA, Ghazy EW, Elbialy ZI, Gaber AA, Hassan AA, Nabil A, Asa SA. Silver nanoparticles induced hepatoxicity via the apoptotic/antiapoptotic pathway with activation of TGFβ-1 and α-SMA triggered liver fibrosis in Sprague Dawley rats. Environmental Science and Pollution Research. 2022;29(53):80448-80465. doi: 10.1007/s11356-022-21388-3.
50. Blanco J, Tomás-Hernández S, García T, Mulero M, Gómez M, Domingo JL, Sánchez DJ. Oral exposure to silver nanoparticles increases oxidative stress markers in the liver of male rats and deregulates the insulin signalling pathway and p53 and cleaved caspase 3 protein expression. Food and Chemical Toxicology. 2018;115:398-404. doi.org/10.1016/j.fct.2018.03.039
51. Moradi-Sardareh H, Basir HR, Hassan ZM, Davoudi M, Amidi F, Paknejad M. Toxicity of silver nanoparticles on different tissues of Balb/C mice. Life sciences. 2018;211:81-90. doi.org/10.1016/j.lfs.2018.09.001
52. Parang Z, Moghadamnia D. Effects of silver nanoparticles on the functional tests of liver and its histological changes in adult male rats. Nanomedicine Research Journal. 2018;3(3):146-53. doi.10.22034/nmrj.2018.03.005
53. Jia R, Cao L, Du J, Xu P, Jeney G, Yin G. The protective effect of silymarin on the carbon tetrachloride (CCl 4)-induced liver injury in common carp (Cyprinus carpio). In Vitro Cellular & Developmental Biology-Animal. 2013 ;49(3):155-61. doi: 10.1007/s11626-013-9587-3
54. Bayader Abdulhadi Abdul Kadhim, Fadhaa Abdulameer Ghafil, Sahar A. Majeed, Heider Qassam, & Najah R. Hadi. Hepato-protective effects of Silymarin against methotrexate-induced hepatotoxicity in rat model. Journal of Population Therapeutics and Clinical Pharmacology. 2013 30(1),373.382. doi.org/10.47750/jptcp.2023.1096
55. Khazaei R, Seidavi A, Bouyeh M. A review on the mechanisms of the effect of silymarin in milk thistle (Silybum marianum) on some

laboratory animals. Veterinary Medicine and Science. 2022;8(1):289-301. doi.org/10.1002/vms3.641

56. Bashandy SA. Beneficial effect of combined administration of vitamin C and vitamin E in amelioration of chronic lead hepatotoxicity. The Egyptian Journal of Hospital Medicine. 2006 ;23(1):371-84. doi: 10.21608/ejhm.2006.17948
57. Phung N, Pera N, Farrell G, Leclercq I, Hou JY, George J. Pro-oxidant-mediated hepatic fibrosis and effects of antioxidant intervention in murine dietary steatohepatitis. International journal of molecular medicine. 2009 ;24(2):171-80. doi.org/10.3892/ijmm_00000220
58. Karimian G, Kirschbaum M, Veldhuis ZJ, Bomfati F, Porte RJ, Lisman T. Vitamin E attenuates the progression of non-alcoholic fatty liver disease caused by partial hepatectomy in mice. PloS one. 2015;10(11):e0143121. doi.org/10.1371/journal.pone.0143121
59. Zaki NT, Al Ankily M, Amin RM, Halawa AM. The possible protective role of vitamin E on the induced silver nanoparticles toxicity on filiform and circumvallate tongue papillae of albino rats histological and immunohistochemical study.JCHR.2021;11(1):63-74.doi:10.22034/jchr.2021/1908602.1172
60. Bakr MM, Al-Ankily MM, Shogaa SM, Shamel M. Attenuating effect of vitamin E against silver nano particles toxicity in submandibular salivary glands. Bioengineering.2021;8(12):219. doi.org/10.3390/bioengineering8120219
61. Lamia SS, Emran T, Rikta JK, Chowdhury NI, Sarker M, Jain P, Islam T, Gias ZT, Shill MC, Reza HM. Coenzyme Q10 and silymarin reduce CCl4-induced oxidative stress and liver and kidney injury in ovariectomized rats—implications for protective therapy in chronic liver and kidney diseases. Pathophysiology.2021;28(1):50-63. doi.org/10.3390/pathophysiology28010005
62. Shotop YM, Al-Suwiti IN. The possible role of vitamins E and C in reducing the toxicity of copper nanoparticles in the kidney and liver of the rats (Rattus norvegicus). Journal of King Saud University-Science.2021;33(2):101357. doi.org/10.1016/j.jksus.2021.101357
63. Abo-EL-Sooud K, Abd-El Hakim YM, Hashem MM, El-Metwally AE, Hassan BA, El-Nour HH. Restorative effects of gallic acid against sub-chronic hepatic toxicity of co-exposure to zinc oxide nanoparticles and arsenic trioxide in male rats. Heliyon. 2023 ;9(6). doi.org/10.1016/j.heliyon.2023.e17326
64. Yousof SM, Erfan H, Hosny MM, Shehata SA, El-Sayed K. Subacute toxic effects of silver nanoparticles oral administration and withdrawal on the structure and function of adult Albino Rats' hepatic tissue. Saudi Journal of Biological Sciences. 2022;29(5):3890-8. doi.org/10.1016/j.sjbs.2022.02.054
65. Zielinska E, Zauszkiewicz-Pawlak A, Wojcik M, Inkielewicz-Stepniak I. Silver nanoparticles of different sizes induce a mixed type of programmed cell death in human pancreatic ductal adenocarcinoma. Oncotarget.2018;9(4):4675. doi: 10.18632/oncotarget.22563
66. Patlolla AK, Hackett D, Tchounwou PB. Silver nanoparticle-induced oxidative stress-dependent toxicity in Sprague-Dawley rats. Molecular and cellular biochemistry. 2015 ;399:257-68.doi: 10.1007/s11010-014-2252-7.
67. Bajpai J, Prakash V, Kant S, Verma AK, Srivastava A, Bajaj DK, Ahmad MK, Agarwal A. Study of oxidative stress biomarkers in chronic obstructive pulmonary disease and their correlation with disease severity in north Indian population cohort. Lung India. 2017;34(4):324-9. doi: 10.4103/lungindia.lungindia_205_16
68. Vairetti M, Di Pasqua LG, Cagna M, Richelmi P, Ferrigno A, Berardo C. Changes in glutathione content in liver diseases: an update. Antioxidants. 2021;10(3):364.doi.org/10.3390/antiox10030364
69. Abd El-Maksoud EM, Lebda MA, Hashem AE, Taha NM, Kamel MA. Ginkgo biloba mitigates silver nanoparticles-induced hepatotoxicity in Wistar rats via improvement of mitochondrial biogenesis and antioxidant status. Environmental Science and Pollution Research.2019;26(25):25844-25854.doi: 10.1007/s11356-019-05835-2.
70. Atiba AS, Abbiyesuku FM, Oparinde DP, Temitope A, Akindele RA. Plasma malondialdehyde (MDA): an indication of liver damage in women with pre-eclamsia. Ethiopian journal of health sciences. 2016;26(5):479-86. doi:10.4314/ejhs.v26i5.10